HEFAT2012
9th International Conference on Heat Transfer, Fluid Mechanics and Thermodynamics
16 – 18 July 2012
Malta

HEAT TRANSFER AND PRESSURE DROP IN MICROCHANNELS WITH DIFFERENT INLET CONDITIONS FOR WATER IN THE LAMINAR AND TRANSITIONAL REGIMES

Garach D.V., Dirker J.* and Meyer J.P.
*Author for correspondence
Department of Mechanical and Aeronautical Engineering,
University of Pretoria,
Pretoria, 0002,
South Africa,
E-mail: jaco.dirker@up.ac.za

ABSTRACT

Heat transfer by means of microchannels is an efficient method of cooling small but high-heat-dissipating objects. With very high heat transfer coefficients, the application of microchannels, especially in the field of electronics cooling, shows potential. With the aid of different inlet conditions, an experimental investigation to measure the heat transfer and pressure drop in a single copper microchannel, with a constant surface heat flux boundary condition, was undertaken in the laminar, transitional, and early turbulent regimes. Three test sections of hydraulic diameters 1.05 mm, 0.85 mm and 0.57 mm and of equal lengths of 200 mm were experimentally investigated using two inlet conditions: a sudden contraction inlet and a bellmouth inlet. Friction factors were determined for three heat input conditions per test section. Results show lower values of the friction factor than the conventional theory in the laminar and turbulent regimes for the sudden contraction inlet. The bellmouth inlet results show an early onset of transition compared to the sudden contraction, with a longer and smoother transition profile. Nusselt number results were higher in the laminar regime, while increasing until the onset of transition. Turbulent results show convergence to the Gnielinski equation for both inlet conditions.

INTRODUCTION

Heat transfer in microchannels has been under investigation since the early 1980's, when Tuckerman and Pease [1] first introduced the method of cooling an integrated circuit with an array of rectangular fused silica channels using water as the liquid medium. The interest in microchannels intensified, with more researchers investigating different materials, cross-sectional shapes, fluids, etc. Tuckerman and Pease reported high heat transfer coefficients and stated that the friction factors were well predictable using conventional theory.

NOMENCLATURE

A_s	[m^2]	Wetted channel surface area
D_h	[m]	Hydraulic diameter
C_p	[J/kgK]	Specific heat of fluid
eb	[-]	Energy balance
f	[-]	Friction factor
$\bar{h}$	[W/m^{2}K]	Average heat transfer coefficient
H	[m]	Microchannel height
j	[-]	Colburn j-factor
k	[W/mK]	Thermal conductivity
L_p	[m]	Differential pressure length
$\dot{m}$	[kg/s]	Fluid mass flow rate
$\overline{Nu}$	[-]	Average Nusselt number
Pr	[-]	Prandtl number
$\bar{Q}_{in}$	[W]	Power input
$\bar{Q}_{out}$	[W]	Heat transferred to water
Re	[-]	Reynolds number
$\bar{T}_b$	[K]	Average bulk fluid temperature
$\bar{T}_{in}$	[K]	Average fluid inlet temperature
$\bar{T}_{out}$	[K]	Average fluid outlet temperature
$\bar{T}_w$	[K]	Average wall temperature
v	[m/s]	Average fluid velocity
W	[m]	Microchannel width

Special characters

α	[-]	Microchannel aspect ratio
ΔP	[Pa]	Differential pressure
ρ	[kg/m^3]	Fluid density

Subscripts

sl	Shah and London correlation
bl	Blasius correlation

Peng and Peterson [2] thereafter experimentally tested multiport microchannels. Their experiments utilized stainless steel channels rather than the fused silica used in the work of Tuckerman and Pease. With rectangular channels, and using water as their working fluid, they reported that the measured friction factor was either lower than the conventional theory, or higher, depending on the hydraulic diameter. They proposed a correlation to predict the pressure drop along the length of a microchannel. Similarly, they noticed deviations in their Nusselt number values, and proposed correlations for both the laminar and turbulent regimes. Their results indicated that transition to turbulence occurred between a Reynolds number of 2 000 and 3 000.

Weilin *et al.* [3] experimentally measured the pressure drop along the length of trapezoidal shaped microchannels manufactured from fused silica. With an adiabatic boundary condition, they reported an increase in friction factor over the conventional theory for microchannels smaller than 0.17 mm. They were one of the first to also report on the microchannel relative surface roughness, measuring values between 1.24% and 1.75%. Reporting that the friction factor deviates at a Reynolds number of 500, they suggested that the deviation is due to the surface roughness, and proposed a roughness-viscosity model to predict the pressure drop in a microchannel.

Judy *et al.* [4] experimentally tested water, methanol and isopropanol in square and circular channels manufactured from fused silica and stainless steel. They ran their experiments under adiabatic conditions for microchannels with diameters varying from 0.015 mm to 0.15 mm. They did not report on their surface roughness, but found good agreement of the friction factor to conventional theory. Their experiments were conducted in the laminar regime and they noticed that the onset of transition occurred at a Reynolds number of 2 000 for the stainless steel test section.

Celeta *et al.* [5], in 2004, conducted experiments on circular channels manufactured from fused silica. A constant surface temperature boundary condition was used and the added heat was removed with water. They reported mixed results, with both equal and increased friction factor measurements for channels of hydraulic diameters between 0.08 mm to 0.17 mm. The transitional regime occurred between a Reynolds number of 1 900 and 2 500 with turbulent flow following thereafter. The Nusselt number was reported to deviate in the laminar regime and was correlated in the turbulent regime using the turbulent Gnielinski equation (9). They reported a relative surface roughness less than 0.1%.

Hao *et al.* [6] conducted experiments on water in a trapezoidal fused-silica channel of diameter 0.24 mm. Running adiabatic experiments, they measured the pressure drop along the length of a single microchannel. They concluded that conventional theory can predict the friction factor behaviour for values of Reynolds number lower than 1 400, noting that transition occurred between 1 500 and 1 800. Their relative surface roughness was measured at 0.03%.

Steinke and Kandlikar [7] conducted experiments on a multiport microchannel test section in the laminar regime with water. Their test section consisted of twenty six 0.20 mm x 0.25 mm rectangular channels, and adiabatic experiments were conducted. Experimentally testing to a Reynolds number of 800, they noticed that the friction factors would increase unpredictably after a Reynolds number of 300. By correcting for developing flow, they reduced the high deviation from the conventional theory. They then documented the measured friction factor at 33% higher than what the conventional theory predicted. They reported that the uncertainty in microchannels is very high with regards to inlet/exit pressure losses and channel geometry, and put emphasis for future work on the accurate measurement of geometric details.

Natrajan and Christensen [8] experimented on a single copper microchannel and varied the wall surface roughness. This was done using replaceable channel walls of different roughnesses. Using a 0.6 mm rectangular channel, they conducted both friction factor and Nusselt number measurements, concluding that both are well predictable by conventional theory. Their results show that by increasing the surface roughness, the critical Reynolds number reduced from 1 800 to 1 300. Full turbulence occurred thereafter between Reynolds numbers of 2 300 and 2 700 depending on the surface roughness of the experiment.

The results of past research show very mixed outcomes, with authors publishing both conforming and un-conforming results with respect to the friction factor and Nusselt number. The effect of inlet conditions is investigated in the current study, and a comparison of the friction factor, critical Reynolds number and Nusselt number for three single copper test sections is completed using water as the fluid medium.

EXPERIMENTAL FACILITY AND SETUP

Test facility layout and operation

A test facility was designed and constructed for the microchannel test sections. A closed-loop system was designed as shown in Figure 1. Water was supplied from a reservoir where it passed through a 15 µm filter before it reached the pump. An *Ismatec BVP-Z standard* analogue gear pump was used to provide pulseless flow at low flow rates. Water was pumped through a *CMF10 Micro Motion* coriolis mass flow meter where the mass flow rate was measured.

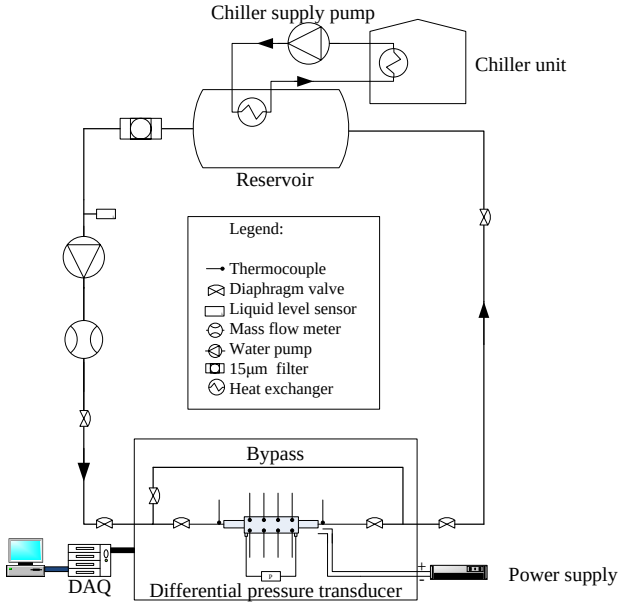

Figure 1 Schematic of microchannel test facility

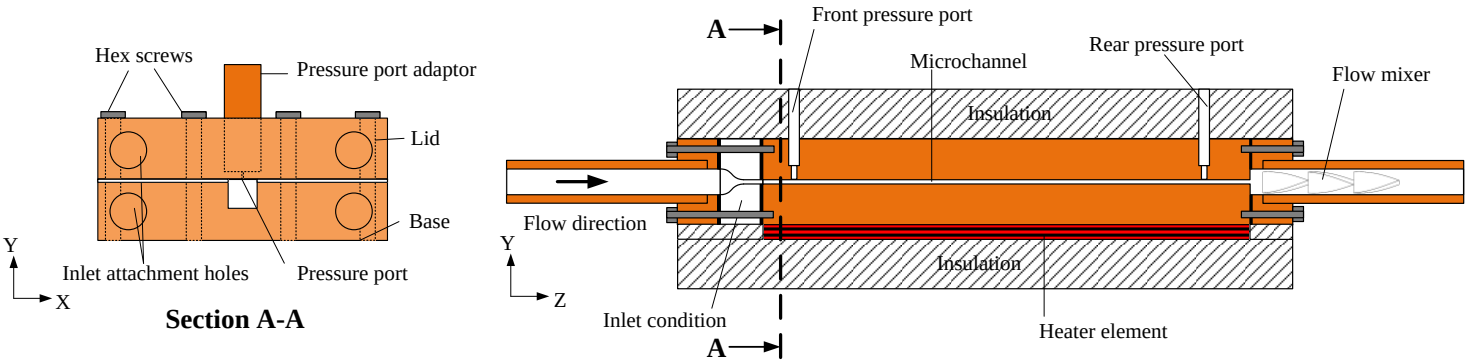

Figure 2 Assembly view of test section

The water then reached the test section where a power input was supplied to a heater element located below the test section. A *Kikusui PWR800M* D.C. power supply provided a constant power to the heater element. The heated water thereafter entered the reservoir where it was cooled using an embedded coiled heat exchanger supplied by chilled water from the laboratory chiller unit. The cooled water in the reservoir then re-entered the system loop to be pumped through the system.

A liquid level sensor was placed before the pump to detect any air particles in the water. The pump was automatically switched off if particles were detected.

Test section design, construction and assembly

Three copper test sections having hydraulic diameters of 1.05 mm, 0.85 mm and 0.57 mm were manufactured. Each had a length of 200 mm. Square channels were machined in copper bars, with eight perpendicular slots placed close to the channel wall to hold the wall thermocouples (see Figure 3). The relative surface roughnesses were measured to be 0.84% for the 0.57 mm test section, 0.32% for the 0.85 mm test section, and 0.23% for the 1.05 mm test section.

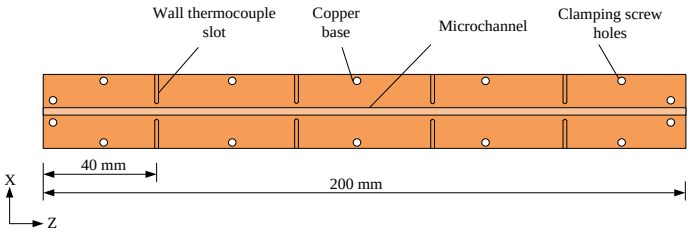

Figure 3 Microchannel test section base design

Threaded holes were drilled into the test section to allow the lid to be clamped to the microchannel base material. The lid was kept common for all three test sections. Two 0.1 mm pressure ports were located along the mid-plane of the lid, 5 mm from each end (in the middle of the microchannel top wall – see Figure 2). Copper pressure port adapters were placed in the lid to allow for easy connection between the test section and the pressure transducer.

A *Validyne DP15* pressure transducer was used to measure the pressure drop inside the microchannel. A total differential pressure length of 190 mm was used to measure the pressure difference in the channel. Two diaphragm gauges (#34 and #44) were used to determine the pressure drop in the test sections each with its own range and uncertainty. Eight T-type thermocouples were used to measure the wall temperature of the test section; four on each side of the side walls (see Figure 3). The temperatures at each location were averaged, and four wall temperature measurements were used to determine the wall temperature. Four inlet and four outlet thermocouples were used to measure the inlet and outlet temperatures. Both measurement points were insulated from the test section to prevent heat conducting from the heater element through the material to the temperature measurement locations.

A flow calmer was placed before the test section to reduce flow inconsistency after the pump. A flow mixer was placed after the test section and before the outlet temperature measurement location to enhance the mixing before the water was measured. This reduced the thermal gradient that existed in the laminar regime experimentation, resulting in a more accurate average outlet temperature measurement.

The test section assembly was sealed by placing 2 layers of PTFE tape between the base and lid for each test section. Once positioned, the lid was attached using fourteen hex screws. The PTFE layer ensured that there were no leaks between the base and the lid and was measured at 50µm in thickness. Figures 4 *(a.)* to *(d.)* show the assembly process. The wall thermocouples were inserted prior to the assembly process.

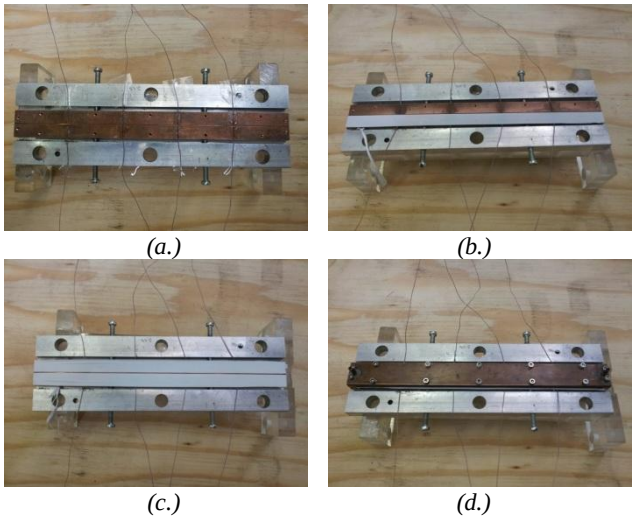

Figure 4 **(***a.)* Attachment of wall thermocouples, **(***b.)* Placing of first PTFE layer, **(***c.)* 2nd layer complete, **(***d.)* Assembled test section

Inlet condition design

Two inlet section types were considered for the comparison of the impact of inlet conditions on microchannel flow - a sudden contraction and a bellmouth inlet condition.

The sudden contraction inlet condition contracted the system piping to the microchannel as depicted in Figure 5*(a.)*. The bellmouth inlet section was designed according to the method prescribed by Morel [9] and is depicted in Figure 5*(b.)*. The bellmouth inlet section was manufactured from perspex in two halves which were joined by an adhesive layer. The material prevented heat conduction from the copper and resulted in semi-adiabatic inlet sections.

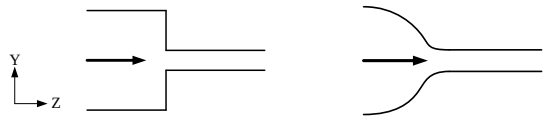

Figure 5 (*a.)* Sudden contraction inlet, (*b.)* Bellmouth inlet

The inlets were aligned to the test section to ensure correct positioning before attachment. The test section was thereafter attached to the system using copper connector pipes.

DATA REDUCTION AND UNCERTAINTY ANALYSIS

Experimentation was done in the laminar, transition and early turbulent regimes. Data was logged for a Reynolds number ranging from 300 up to 2 800. The data logging took place at steady state conditions, determined by the measured energy balance, given by equation (1). When the variation of the energy balance was within ±5% of the displayed value, and there was no variation in the bulk, wall and insulation temperatures, and mass flow rate, the data was logged.

$$eb = \frac{\bar{Q}_{in} - \bar{Q}_{out}}{\bar{Q}_{in}} \tag{1}$$

$\bar{Q}_{in}$ is the measured power input value from the power supply, and $\bar{Q}_{out}$ is the heat transferred to the fluid, calculated using equation (2). The eb can range from 0 – 1, where 0 refers to no heat transfer and 1 refers to heat transfer with no losses. Data was logged when the eb value was constant for a time period of approximately 2 minutes, and not increasing/decreasing, or fluctuating wildly. On average, there were 4% losses, and so the data was logged when the eb stabilized to approximately 0.96.

$$\bar{Q}_{out} = \dot{m} C_p (\bar{T}_{out} - \bar{T}_{in}) \tag{2}$$

Once logged and the calibration applied to the thermocouple measurements, the water properties were calculated using the equations prescribe by Popiel and Wojtkowiak [10]. These properties were determined using the mean bulk fluid temperatures calculated from the inlet and outlet temperature measurements. Using the measured differential pressure, mass flow rate and mean bulk fluid temperatures, the measured friction factor was calculated using equation (3).

$$f = \Delta P \frac{D_h}{L_p} \frac{2}{\rho v^2} \tag{3}$$

The heat transfer coefficient was calculated using equation (4), while the Nusselt number was calculated thereafter using equation (5).

$$\bar{h} = \frac{\bar{Q}_{out}}{A_s(\bar{T}_w - \bar{T}_b)} \tag{4}$$

$$\overline{Nu} = \frac{\bar{h} D_h}{k} \tag{5}$$

For the laminar regime, the friction factor was compared to the Shah and London correlation [11] for rectangular channels is given by equation (6).

$$f_{sl} = \frac{96}{Re}(1 - 1.3553\alpha + 1.946\alpha^2 - 1.7012\alpha^3 + 0.9564\alpha^4 - 0.2537\alpha^5) \tag{6}$$

$$\text{where: } \alpha = \frac{\max(W,H)}{\min(W,H)} \tag{7}$$

Turbulent friction factors were compared to the Blasius equation, as is given by equation (8).

$$f_{bl} = 0.3164/Re^{\frac{1}{4}} \tag{8}$$

The laminar Nusselt number was compared to the constant value of 3.61 for square channels under a constant surface heat flux boundary condition at fully developed flow. Turbulent regime Nusselt number results were compared against the Gnielinski equation, given by equation (9).

$$\overline{Nu} = \frac{(f/8)(Re - 1000)Pr}{1 + 12.7\left(\sqrt{f/8}\right)^{\frac{1}{2}}\left(Pr^{\frac{2}{3}} - 1\right)} \tag{9}$$

Using the measured Nusselt number, the Colburn j-factor, equation (10), was calculated for both inlet conditions. The j-factor can be compared to the friction factor due to their similar profile shapes.

$$j = \frac{\overline{Nu}}{RePr^{\frac{1}{3}}} \tag{10}$$

Results amongst test sections were comparable to each other due to the similar channel surface-area-heat-flux conditions applied to the test sections. Three constant heat inputs were applied across the test section bottom surface, as given in Table 1.

D_h	*Heat Input [W]*		
1.05 mm	20	30	40
0.85 mm	16	24	32
0.57 mm	10	15	20

Table 1 Constant heat input for each test section

Inlet and outlet temperatures were calculated taking the average values, while the trapezoidal rule was employed to determine the wall temperature accurately. The two differential pressure transducer diaphragms captured the results of the differential pressure.

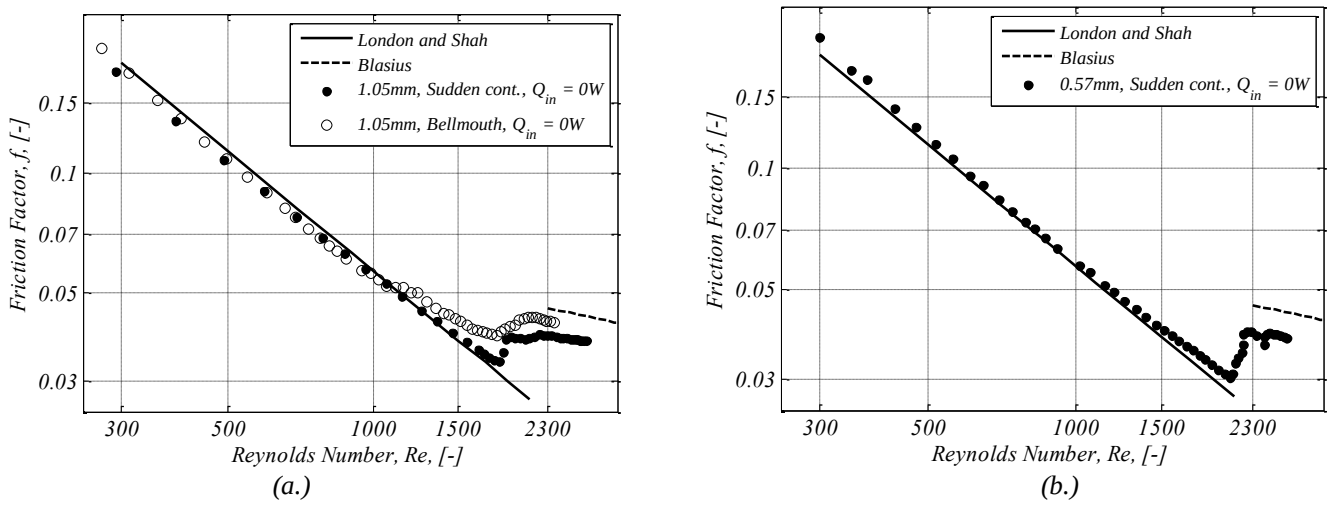

Figure 6 Adiabatic friction factors for: (*a.)* 1.05mm sudden contraction and bellmouth inlet, (*b.)* 0.57mm sudden contraction inlet

		Relative Uncertainty (±)		
Instrument	*Uncertainty*	*Max.*	*Min.*	*Ave.*
Pressure transducer	±57.58 Pa (#34)	8.23%	0.29%	1.85%
	±435.56 Pa (#44)	12.44%	0.27%	1.67%
Thermocouples	±0.1 °C	0.50%	0.18%	0.43%
Mass flow meter	±2.27e-5 kg/s	52%	0.1%	7.54%

Table 2 Equipment uncertainties and operating range

Uncertainties for the mass flow rate, temperature measurements and the differential pressure are given in Table 2. The uncertainties of the friction factor, Reynolds number, Nusselt number and Colburn j-factor were calculated using the methods prescribed by Moffat [12].

The friction factor uncertainty ranged from 46% at a Reynolds number of 300 to 3% at a Reynolds number of 2 800. Nusselt number uncertainties ranged between 7% and 45%, and were dominated by high mass flow meter uncertainties at low Reynolds numbers and low bulk-fluid temperature-to-wall-temperature difference uncertainties at high Reynolds numbers. Mass flow meter uncertainty decreased logarithmically and converged to the minimum uncertainty value (see Table 2) when the mass flow rate was above 5% of the full scale value of 0.0227 kg/s.

RESULTS AND DISCUSSION

Data was logged and analysed for the experiments in the laminar, transition and early turbulent regimes. The results for only the 1.05 mm and 0.57 mm are presented in this paper for adiabatic friction factors, diabatic friction factors, Nusselt numbers and j-factors. Results for the 0.85 mm channel were found to be similar.

Adiabatic results

Data was first captured for the adiabatic results to determine the sensitivity of the pressure transducer, to visualize the effect of the inlet condition before diabatic testing, and to compare the diabatic results to and determine the effect of adding a thermal boundary condition. The effects of the inlet conditions were experimentally investigated in the 1.05 mm test section only for adiabatic experimentation.

Figure 6*(a.)* plots the adiabatic friction factors for the 1.05 mm for the sudden contraction and bellmouth inlet sections. Figure *6(b.)* shows the results for the 0.57 mm sudden contraction inlet section.

Results show good agreement to the Shah and London correlation (6) for rectangular channels for both cases in the laminar regime. The friction factor in the transition regime for the bellmouth inlet condition results increase from 5% to 20% with respect to the sudden contraction inlet condition for a Reynolds number range from 1 150 to 2 300. The results show an early transition occurring with the bellmouth inlet, and a smoother profile of the transition regime compared to the sudden contraction transition regime results. This is opposite to what was found by Olivier and Meyer [13-15] for macro-channels, where the bellmouth delayed the transition regime, which commenced at a much higher Reynolds number

The results in the turbulent regime were over-predicted by the Blasius equation (8) by approximately 10%.

Diabatic results

Diabatic results are given in Figure 7 (*a.)* to (*f.*) The results of the friction factors were compared to the Shah and London correlation (6). The results show slightly lower values for the friction factor. Also noted is an effect of the power input on the friction factor, between 5% and 10%. As the heat input was increased, a lower friction factor was measured. This occurred in the laminar regime and was not observed in the turbulent regime. Turbulent regime results show convergence to the same values for the different inlets, and it is noted that the Blasius equation (8) over predicts the friction factor by approximately 14%.

The effect of the decreasing friction factor due to the heat input is observed for both inlet conditions.

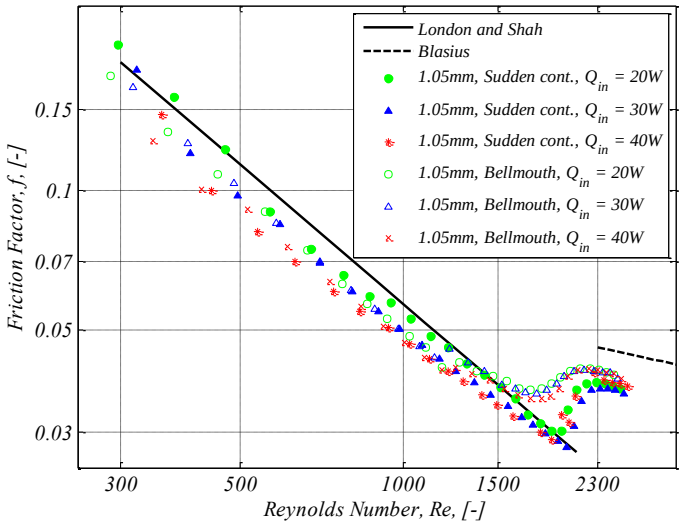

(a.)

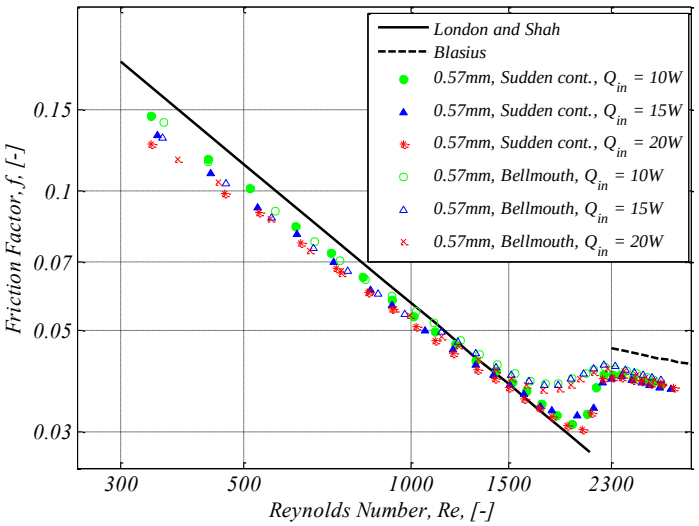

(d.)

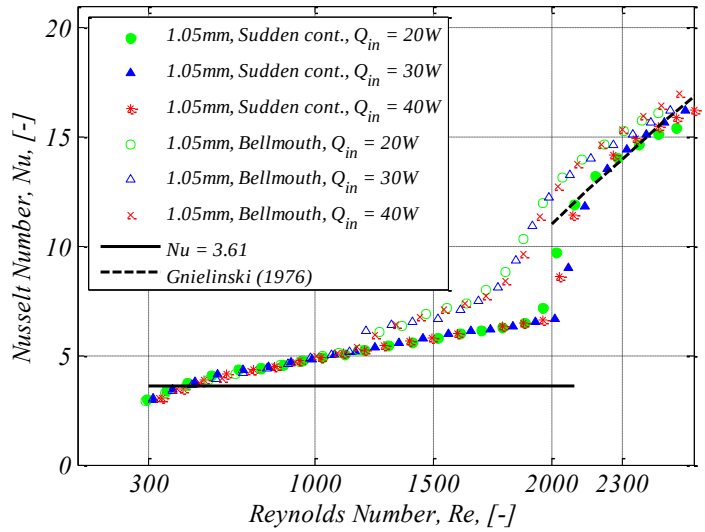

(b.)

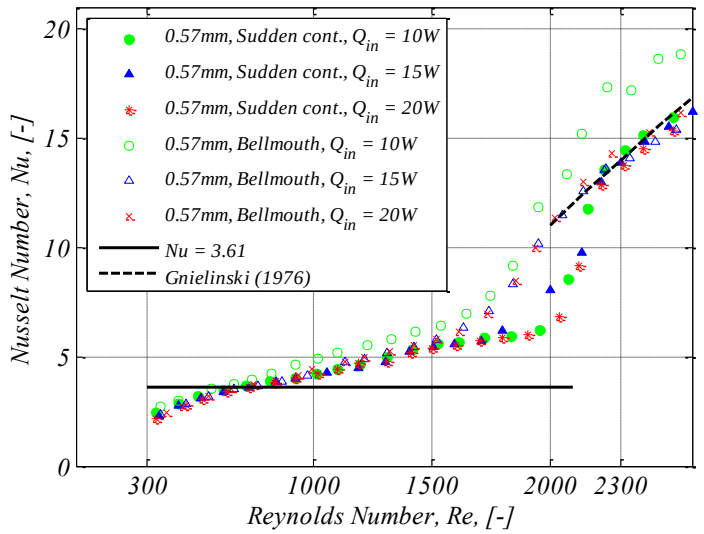

(e.)

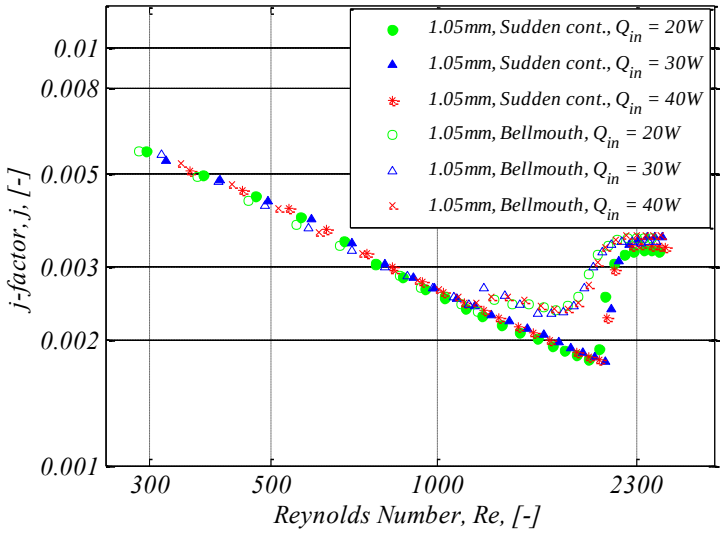

(c.)

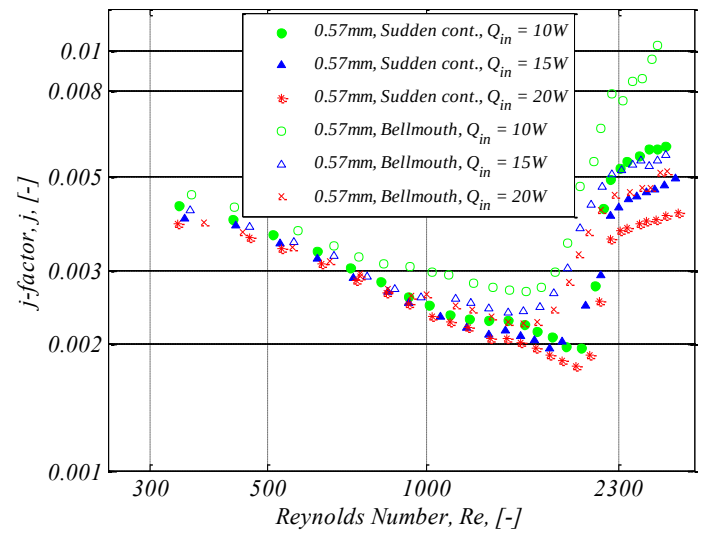

(f.)

Figure 7 Diabatic results for: (*a.)* 1.05 mm friction factors, (*b.)* 1.05 mm Nusselt numbers, *c.* 1.05mm j-factors, (*d.)* 0.57 mm friction factors, (*e.)* 0.57 mm Nusselt numbers, (*f.)* 0.57 mm j-factors, for both the sudden contraction and bellmouth inlet conditions

The critical Reynolds number occurred at approximately 2 000 for all three heat inputs for the sudden contraction inlet condition for both test section diameters.

The bellmouth inlet condition results for the friction factor show similar effects to that of the adiabatic results. Transition commenced earlier at a Reynolds number of approximately 1 700, compared to 2 000 with the sudden contraction inlet. The profile of the transition regime is not as short as the sudden contraction inlet condition, but rather has a smoother transition profile. The turbulent regime for both inlets ended at a Reynolds number of approximately 2 300, where the turbulent regime commenced. The diabatic results can also be compared to the work of Olivier and Meyer [13-15], where their diabatic transition regime results were delayed as with their adiabatic results.

The Nusselt number increased in the laminar regime until transition began. This was attributed to the fact that the flow was developing throughout the laminar regime and could not converge to the constant analytical value of 3.61. There was a dip at the low Reynolds number values, determined to be the effect of the axial heat conduction as discussed by Maranzana *et al.* [16]. Transition occurred at a Reynolds number of 2 000 for the sudden contraction inlet. The bellmouth inlet condition results show a sudden increase in the Nusselt number at a Reynolds number of 1 350. This increase is more noticeable in the 1.05 mm test section, but is also present in the 0.57 mm test section.

For both test sections, the results show an enhancement of the transition regime that begins at an early Reynolds number of approximately 1 350. The transition profile behaved similarly to the friction factor results. The turbulent regime results converged to the Gnielinski equation (9) for most test cases.

The j-factor results were plotted to show the effect of the Nusselt number while taking the Prandtl number variation into consideration. The results show the enhancement effect of the bellmouth inlet condition, especially for the 1.05 mm test section. The effect is also present in the 0.57 mm test section results.

Measurement uncertainties dominated the results at low and high values of Reynolds number. Low mass flow rates (at low Reynolds numbers) increased the mass flow rate measurement uncertainty, while low wall-to-bulk-fluid temperature differences resulted in high measurement uncertainty in the turbulent regime. Since the wall temperature converged towards the bulk fluid temperature in the turbulent regime, higher uncertainties with these measurements were observed.

Due to the effect of the inlet conditions in the transition regime, there is an enhancement of both the friction factors and Nusselt numbers. The results show that there is an increase in the friction factor between 5% and 30% and an increase in the Nusselt number from 10% up to 60% for a Reynolds number between 1 300 and 2 100. This enhancement shows great potential with respect to heat transfer improvement, where there is a high increase on heat transfer rate with a small increase in the friction factor. Effectively, the heat transfer rate increase is more dominant than that of the friction factor, favouring a more efficient operating region for heat transfer applications.

Similar results and effects were determined for the 0.85 mm results for the sudden contraction and bellmouth inlet conditions for the friction factor, Nusselt number and j-factors results.

CONCLUSION

The effects of inlet conditions were experimentally investigated for single copper microchannels with a constant surface heat flux boundary condition.

The Nusselt number and friction factors were determined for three microchannel hydraulic diameters of 1.05 mm, 0.85 mm and 0.57 mm. Friction factor results show good agreement to the conventional theory for adiabatic conditions. Diabatic results show a decrease in the friction factor from the Shah and London correlation. It was found that an increase in the heat input causes a reduction in the friction factor in the laminar regime, and that this effect should be further investigated.

The measured turbulent friction factor results were lower with respect to the Blasius equation which over-predicted them by approximately 14%.

Laminar Nusselt number results did not converge to the constant value of 3.61, but increased in an almost linear fashion. This was attributed to the flow not being fully developed. The effect of the axial heat conduction became more dominant in the laminar regime, and was observed in the steeper gradient in results located between a Reynolds number of 300 and 800. This resulted in lower Nusselt number values. Turbulent regime Nusselt number results showed convergence to the Gnielinski equation.

The Colburn j-factor results were determined and presented, and the effect of changing inlet conditions was visible in the results.

The sudden contraction and bellmouth inlet conditions showed varying results when attached to the same test sections, especially in the transition regime. The bellmouth inlet exhibited Nusselt numbers approximately 10% to 50% higher than the sudden contraction inlet for Reynolds numbers between 1 300 and 2 100. Bellmouth friction factors in the same Reynolds number range were between 5% and 30% higher when compared to the sudden contraction inlet. Further research into inlet conditions will provide more insight into their effect on the transition regime.

REFERENCES

[1] D. Tuckerman and F. Pease, "High-performance heat sinking for VLSI", *IEEE Electron Device Letters*, Vols. EDL-2, no. 5, pp. 126-129, 1981.

[2] X. Peng and G. Peterson, "Convective heat transfer and flow friction for water flow in microchannel structures", *International Journal of Heat and Mass Transfer*, vol. 39, no. 12, pp. 2599-2608, 1996.

[3] Q. Weilin, G. Mala and L. Dongqing, "Pressure-driven water flows in trapezoidal silicon microchannels", *International Journal of Heat and Mass Transfer*, vol. 43, pp. 353-364, 2000.

[4] J. Judy, D. Maynes and B. Webb, "Characterization of frictional pressure drop for liquid flows through

microchannels", *International Journal of Heat and Mass Transfer*, vol. 45, pp. 3477-3489, 2002.

[5] G. Celata, M. Cumo and G. Zummo, "Thermal-hydraulic characterisatics of single-phase flow in capillary tubes", *Experimental Thermal and Fluid Science*, vol. 28, pp. 87-95, 2004.

[6] P. Hao, F. He and K. Zhu, "Flow characteristics in a trapezoidal silicon microchannel", *Journal of Micromechanics and Microengineering*, vol. 15, pp. 1362-1368, 2005.

[7] M. Steinke and S. Kandlikar, "Single-phase liquid friction factors in microchannels", *International Journal of Thermal Sciences*, vol. 45, pp. 1073-1083, 2006.

[8] V. Natrajan and K. Christensen, "Non-intrusive measurements of convective heat transfer in smooth- and rough-wall microchannels: laminar flow", *Journal of Experimental Fluids*, 2010.

[9] T. Morel, "Comprehensive design of axisymmetric wind tunnel contractions", *Journal of Fluids Engineering*, vol. 97, pp. 225-233, 1975.

[10] C. Popiel and J. Wojtkowiak, "Simple formulas for thermophysical properties of liquid", *Heat Transfer Engineering*, vol. 19, no. 3, pp. 87-101, 1998.

[11] R. Shah and A. London, Laminar flow forced convection in ducts, New York: Academic Press, 1978, pp. 196-222.

[12] R. Moffat, "Describing the uncertainties in experimental results", *Experimental Thermal and Fluid Science*, vol. 1, pp. 3-17, 1988.

[13] J. Meyer and J. Olivier, "Transitional flow inside enhanced tubes for fully developed and developing flow with different types of inlet disturbances: Part I - adiabatic pressure drop", *International Journal for Heat and Mass Transfer*, vol. 54, no. 7-8, pp. 1587-1598, 2011.

[14] J. Meyer and J. Olivier, "Transitional flow inside enhanced tubes for fully developed and developing flow with different types of inlet disturbances: Part II - heat transfer", *International Journal for Heat and Mass Transfer*, vol. 54, no. 7-8, pp. 1598-1607, 2011.

[15] J. Olivier and J. Meyer, "Single-phase heat trnasfer and pressure drop of the cooling of water inside smooth tubes for trasnitional flow with different inlet geometries (RP-1280)", *HVAC&R Journal*, vol. 16, no. 4, pp. 471-496, 2010.

[16] G. Maranzana, I. Perry and D. Maillet, "Mini- and micro-channels: influence of axial conduction in the walls", *International Journal of Heat and Mass Transfer*, vol. 47, pp. 3993 - 4004, 2004.